

Quantum state tomography of a fiber-based source of polarization-entangled photon pairs

J. Fan, M. D Eisaman and A. Migdall

Optical Technology Division, National Institute of Standards and Technology
100 Bureau Drive, Mail Stop 8441, Gaithersburg, MD 20899-8441

and

Joint Quantum Institute, University of Maryland, College Park, MD 20742

Jfan@nist.gov

<http://www.opticsexpress.org>

Abstract: We report an experimental demonstration of a bright high-fidelity single-mode-optical-fiber source of polarization-entangled photon pairs. The source takes advantage of single-mode fiber optics, highly nonlinear microstructure fiber, judicious phase-matching, and the inherent stability provided by a Sagnac interferometer. With a modest average pump power (300 μ W), we create all four Bell states with a detected two-photon coincidence rate of 7 kHz per bandwidth of 0.9 nm, in a spectral range of more than 20 nm. To characterize the purity of the states produced by this source, we use quantum-state tomography to reconstruct the corresponding density matrices, with fidelities of 95 % or more for each Bell state.

©2007 Optical Society of America

OCIS codes: (060.4370) Nonlinear optics, fibers; (190.4380) Nonlinear optics, four wave mixing; (190.5650) Raman effect.

References and links

1. E. Schrödinger, "Die gegenwärtige Situation in der Quantenmechanik," *Naturwissenschaften* **23**, 807–812; 823–828; 844–849 (1935).
2. R. P. Feynman, R. B. Leighton, R. B. and M. L. Sands, *The Feynman Lectures on Physics, Vol. 3* (Addison-Wesley, Massachusetts, 1965).
3. C. H. Bennett and G. Brassard, in Proc. IEEE Intl. Conf. on Computers, Systems and Signal Processing 175–179 (IEEE, Bangalore, 1984).
4. A. K. Ekert, "Quantum cryptography based on Bell's theorem," *Phys. Rev. Lett.* **67**, 661–663 (1991).
5. C. H. Bennett, G. Brassard, C. Crepeau, R. Jozsa, A. Peres, and W. K. Wootters, "Teleporting an unknown quantum state via dual classical and Einstein-Podolsky-Rosen channels," *Phys. Rev. Lett.* **70**, 1895–1899 (1993).
6. P. Shor, in Proc. 37th Symp. on Foundations of Computer Science 15–65 (IEEE Computer Society Press, Los Alamitos, 1996).
7. N. Gisin, G. Ribordy, W. Tittel, and H. Zbinden, "Quantum cryptography," *Rev. Mod. Phys.* **74**, 145–195 (2002).
8. J. F. Clauser, in *Quantum [Un]speakables: From Bell to Quantum Information*, R. A. Bertlmann, and A. Zeilinger, eds., (Springer, Heidelberg, 2002) pg. 61–98.
9. M. A. Nielsen and I. L. Chung, *Quantum Computation and Quantum Information*, (Cambridge University Press, 2000).
10. D. Bouwmeester, J. W. Pan, K. Mattle, M. Eibl, H. Weinfurter, and A. Zeilinger, "Experimental quantum teleportation," *Nature* **390**, 575–579 (1997).
11. P. Walther, K. J. Resch, T. Rudolph, E. Schenck, H. Weinfurter, V. Vedral, M. Aspelmeyer, A. Zeilinger, "Experimental one-way quantum computing," *Nature* **434**, 169–176 (2005).
12. N. Gisin and R. Thew, "Quantum Communication," *Nat. Photonics* **1**, 165–171 (2007).
13. D. C. Burnham and D. L. Weinberg, "Observation of simultaneity in parametric production of optical photon pairs," *Phys. Rev. Lett.* **25**, 84–87 (1970).
14. P. G. Kwiat, E. Waks, A. G. White, I. Appelbaum, and P. H. Eberhard, "Ultrabright source of polarization-entangled photons," *Phys. Rev. A* **60**, 773–776 (R) (1999).
15. C. Kurtsiefer, M. Oberparleiter and H. Weinfurter, "High-efficiency entangled photon pair collection in type-II parametric fluorescence," *Phys. Rev. A* **64**, 023802 1–4 (2001).

16. J. Altepeter, E. Jeffrey, and P. G. Kwiat, "Phase-compensated ultra-bright source of entangled photons," *Opt. Express* **13**, 8951-8959 (2005).
17. T. Kim, M. Fiorentino, and F. N. C. Wong, "Phase-stable source of polarization-entangled photons using a polarization Sagnac interferometer," *Phys. Rev. A* **73**, 012316 (2006).
18. G. P. Agrawal, *Nonlinear Fiber Optics*, 2nd edition (Academic, New York, 1995).
19. L. J. Wang, C. K. Hong, and S. R. Friberg, "Generation of correlated photons via four-wave mixing in optical fibres," *J. Opt. B: Quantum Semiclass. Opt.* **3**, 346-352 (2001).
20. H. Takesue, and K. Inoue, "Generation of polarization-entangled photon pairs and violation of Bell's inequality using spontaneous four-wave mixing in a fiber loop," *Phys. Rev. A*, **70**, 031802-031804 (R) (2004).
21. X. Li., P. L. Voss, Jay E. Sharping, and P. Kumar, "Optical-fiber source of polarization-entangled photons in the 1550 nm Telecom Band," *Phys. Rev. Lett.* **94**, 053601-053605 (2005).
22. A. Birks, J. C. Knight, and P. St. Russell, "Endlessly single-mode photonic crystal fiber," *Opt. Lett.* **22**, 961-963 (1997).
23. J. Fan, A. Migdall, and L. J. Wang, "Efficient generation of correlated photon pairs in a microstructure fiber," *Opt. Lett.* **30**, 3368-3370 (2005).
24. F. V. Daniel, Paul G. Kwiat, William J. Munro, and Andrew G. White, "On the measurement of qubits," *Phys. Rev. A* **64**, 052312 1-23 (2001).
25. J. Fan, and A. Migdall, "A broadband high spectral brightness fiber-based two-photon source," *Opt. Express* **15**, 2915-2920 (2007).
26. J. Fan, M. D. Eisaman, and A. Migdall, "Bright phase-stable broadband fiber-based source of polarization-entangled photon pairs," *Phys. Rev. A* **76**, 2043836 (2007).

1. Introduction

Entanglement [1], an essential trait of quantum mechanics, together with the superposition principle, has led to new concepts in information technology, resulting in the emergence of quantum-information science [2-9]. Many quantum-information protocols require high-fidelity entangled states, often realized experimentally in the form of polarization-entangled photon pairs [10-12]. Entangled photon pairs typically have been produced by three-wave mixing, where a photon of frequency ω_p is annihilated in a nonlinear crystal to create a pair of photons of lower frequencies (ω_1 and ω_2) with $\omega_p = \omega_1 + \omega_2$, a process referred to as parametric down-conversion [13]. Thirty-seven years of continuous study has yielded a number of bright down-conversion-based entangled photon-pair sources [14-17], yet a serious drawback remains - the photons are emitted into a large number of spatial and spectral modes. Unfortunately, many quantum-information applications require photons in a narrow spectral bandwidth and a single spatial mode.

While these sources have been developing, the communications industry has undergone a revolution: a massive network of single-mode optical fiber has been installed, allowing a truly global exchange of information. To facilitate long-range communications, nonlinear interactions such as four-wave mixing (FWM) and Raman scattering in single-mode optical fiber have been extensively studied in part to avoid their numerous negative effects such as cross-talk and signal loss [18]. On the positive side, it is also possible to use these nonlinearities to one's advantage. For example, FWM in fiber, where two pump photons are annihilated to create a pair of correlated photons (referred to as signal ω_s and idler ω_i , with $2\omega_p = \omega_s + \omega_i$), opens a new possibility that entangled photon pairs can be produced and transmitted for quantum-information processing, all within an optical-fiber network [19].

FWM is the dominant parametric process in single-mode optical fiber because the centrosymmetry of single-mode fiber glass allows no three-wave mixing [18]. The two-photon gain is determined by FWM phase-matching and the effective fiber nonlinear coefficient γ which relates to the Kerr-nonlinearity (n_2) and effective mode area (A_{eff}) as $\gamma = \frac{2\pi n_2}{\lambda A_{\text{eff}}}$. The gain is

proportional to $|\gamma P z|^2$ when the fiber dispersion $(2k_p - k_s - k_i)z$ is cancelled by the Kerr nonlinearity-induced self-phase modulation $2\gamma P z$, (known as perfect phase-matching), $(k_s + k_i - 2k_p)z + 2\gamma P z = 0$, where z is fiber length, P is peak power, and k_p and $k_{s,i}$ are wave numbers for the pump, signal, and idler photons, respectively.

In addition to FWM, pump photons may individually exchange phonons with the fiber glass, resulting in Raman transitions [18]. At room temperature, this Raman scattering presents a broadband single-photon noise background to the two-photon light of interest, with the Raman scattering peak at a $\Delta\omega = 13$ THz ($\Delta\omega = \omega_p - \omega_s$) detuning from the pump laser, and extending over 40 THz (inset 1 of Fig. 1). Previous experimental studies of FWM used conventional fibers possessing a small nonlinear coefficient ($\gamma \approx 1 \text{ W}^{-1}\text{km}^{-1}$), and therefore a low two-photon production probability [20, 21]. In this paper, we report the complete characterization of a bright fiber-based source of polarization-entangled two photon source. We use a highly nonlinear microstructure fiber in the experiment. The microstructure fiber consists of a solid core of glass suspended by a thin web of glass, allowing for a small core diameter and single spatial-mode propagation with low loss for a wide range of wavelengths [22]. With reduced spatial-mode area, the nonlinear coefficient of this fiber, and thus the two-photon production probability, are significantly enhanced. (For example, the microstructure fiber with a core diameter of $1.2 \mu\text{m}$ used in our experiment has $\gamma \approx 70 \text{ W}^{-1}\text{km}^{-1}$ at 740 nm, 70x larger than conventional fiber.) In addition, we phase-match the FWM process with a large detuning to produce correlated signal and idler photons that are outside of the main Raman spectral band, significantly reducing the single-photon noise level. We also introduce new optical arrangements that enhance the source stability and operationally flexibility.

In previous three-wave or four-wave mixing schemes producing entangled photon pairs, two photon pairs ($H_s H_i$ and $V_s V_i$, H : horizontal polarization, V : vertical polarization) were created separately, and then interferometrically combined to be indistinguishable. The need for the two photon pairs to be indistinguishable requires precise spatial-, temporal-, and spectral-mode controls. Achieving this in a three-wave process is possible, but at the cost of flexibility in spectral mode selection [14-16]. Four-wave schemes offer less stability because of temporal coherence drifts between the two pump beams required, but more flexibility in spectral-mode selection [20, 21]. To achieve both source stability and easy spectral selectivity, we introduce a new design that uses a polarization-configured single-mode optical-fiber Sagnac interferometer.

The experimental setup in Fig. 1 shows the principle of the interferometer. We use the fact that in twisting a polarization-maintaining optical fiber gradually, the polarization state of the light simply rotates with the fiber. We orient the fiber principal axis horizontally at one end and vertically at the other end, so that the input H -polarized light beam (from the H -end of the fiber) is output (from the V -end of the fiber) in the V -polarization state, and vice versa. The interferometer is configured with the H -end of the fiber accepting the H -polarized pump beam that is transmitted through the polarizing beam splitter (PBS) and the V -end accepting the V -polarized pump beam that is reflected from the PBS. The PBS acts as an access port for light to be coupled into and out of the Sagnac interferometer. This interferometer design is mechanically robust with no need of dynamic controls such as delay stages. In addition, it is achromatic with no need of optical elements for phase-retarding control.

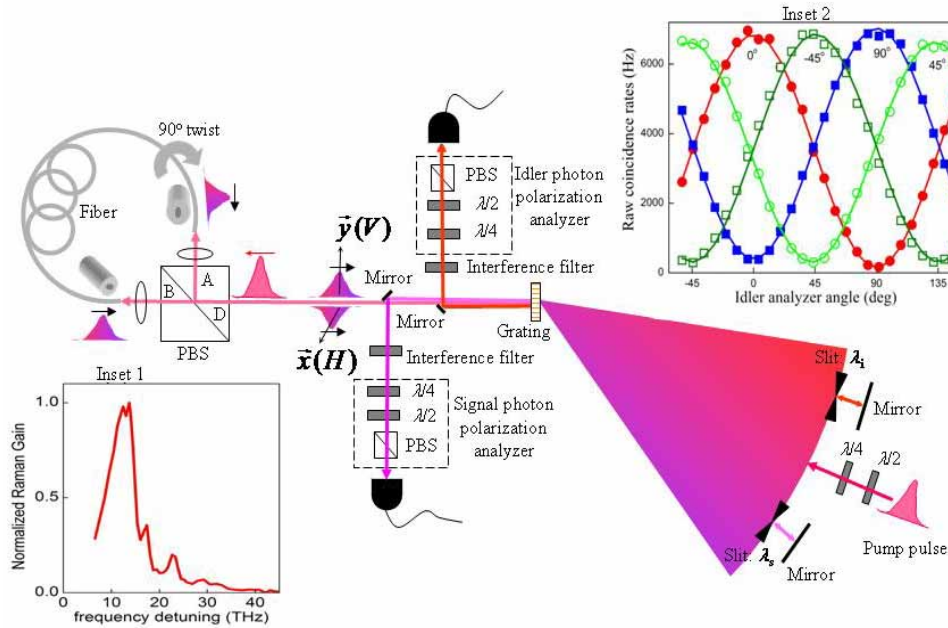


Fig. 1. Experimental setup. After passing through a transmission grating, the 8 ps linearly polarized pump laser pulse ($\lambda_p = 740.7$ nm, repetition rate = 80 MHz) is sent to the Sagnac interferometer via the polarizing beam splitter (PBS). A 1.8 m long polarization-maintaining microstructure fiber is the nonlinear FWM medium with zero-dispersion wavelength $\lambda_{zdw} = 745 \pm 5$ nm and nonlinearity $\gamma = 70$ $W^{-1}km^{-1}$ at λ_p . The H -end of fiber (with principal axis oriented horizontally) faces port B of PBS and the V -end of fiber (with principal axis oriented vertically) faces port A. Inset 1 shows the Raman gain spectral profile of our fibers as a function of detuning from the pump wavelength. Inset 2 shows the measured two-photon quantum-interference fringes for Bell state Φ^- at four angle settings of θ_s for the polarization analyzer in the signal arm: $\theta_s = 0^\circ, 45^\circ, 90^\circ, -45^\circ$ with $\lambda_s = 689.5$ nm, $\lambda_i = 799.5$ nm, $\Delta\lambda = 0.9$ nm. The visibility, $V = (C_{\max} - C_{\min}) / (C_{\max} + C_{\min})$ is calculated with a sine-squared-function-fit, where C_{\max} and C_{\min} are the maximum and minimum coincidence count rates. $\lambda/2$: half-wave plate; $\lambda/4$: quarter-wave plate.

By sending a linearly polarized laser pump pulse (45° oriented respect to the H -axis) into the Sagnac interferometer via the PBS, the equal-power transmitted and reflected components counter-propagate, each driving a FWM process. The cross-polarized equal-power outputs from the two fiber ends are combined at the PBS and exit together into indistinguishable spatial and temporal modes, thus forming the Bell state $\Phi^+(\Delta\omega) = H_s(\Delta\omega)H_i(-\Delta\omega) + V_s(\Delta\omega)V_i(-\Delta\omega)$ with frequency-conjugate signal and idler photon pairs with respect to the pump wavelength λ . With our two-pass grating configuration [23], these polarization-entangled single spatial-mode photon pairs can be selected either in a narrow spectral bandwidth, or in a group of spectral bandwidths by wavelength-division multiplexing.

With a total average pump power of 300 μW , the measured two-photon coincidence rate is 7 kHz with $\lambda_s = 689$ nm, $\lambda_i = 800$ nm, and $\Delta\lambda = 0.9$ nm). The two-photon quantum interferences measured for the Bell state $\Phi^-(\Delta\omega)$ ($\Phi^-(\Delta\omega) = H_s(\Delta\omega)H_i(-\Delta\omega) - V_s(\Delta\omega)V_i(-\Delta\omega)$, $\Delta\omega = 32$ THz) are plotted in inset 2 of Fig. 1, showing high visibility greater than 91 % without subtracting accidentals and greater than 97 % with accidentals subtracted.

To characterize the produced polarization-entangled quantum states, we developed an automatic control system to complete the quantum state tomography measurements [24]. The wave plates in the polarization analyzers of the signal and idler arms are mounted on automatic rotation stages that are computer controlled. Following the procedure described in Ref. 24, the rotation angles for wave plates in 36 angle settings in the $H, V, D = (H + V)/2^{1/2}$ and $R = (H - iV)/2^{1/2}$ bases for the tomography measurement are programmed into the computer. After optical alignment, the program automatically executes the tomography measurements, with 10 seconds of data accumulation time for each setting. The density matrix for each Bell state is reconstructed with the maximum likelihood method, using the two-photon coincidence and accidental events accumulated in these 36 measurements as input. The fidelity (F) of the reconstructed density matrix, ρ , measuring the degree of overlap between the produced state and ideal state, is defined as $\langle \Psi | \rho | \Psi \rangle$, where Ψ represents the Bell state of interest. We measured $F \geq 95\%$ for reconstructed density matrices of all of the four Bell states produced using our fiber-based source.

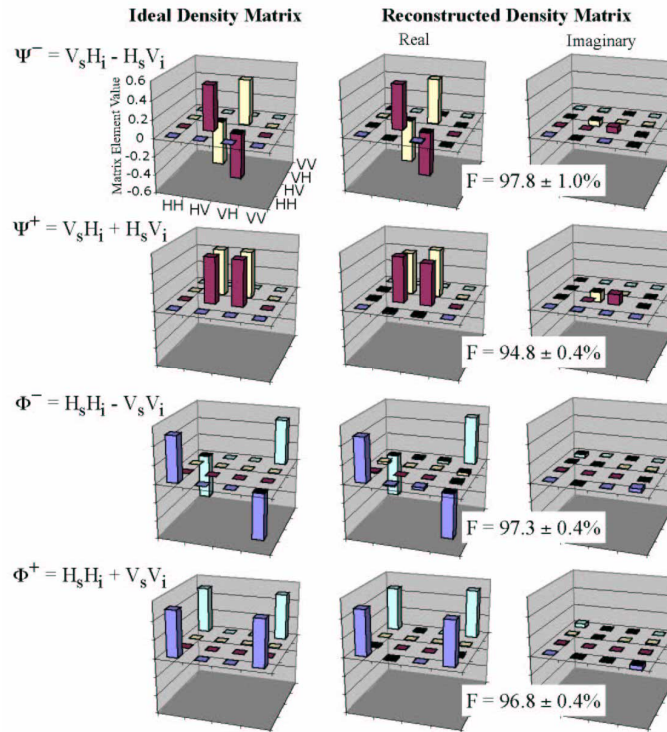


Fig. 2. Density matrix reconstruction of all four Bell states. The ideal density matrix (which is real) and the reconstructed density matrix (real and imaginary parts) are shown for each of the four Bell states with $\lambda_s = 693$ nm and $\lambda_i = 795$ nm, along with the fidelities calculated from the reconstructed matrices.

The two-pass grating configuration allows us to select Bell states at different wavelengths by simply translating the slits to different positions, without performing additional optical alignment, and without reducing the 7 kHz coincidence rate [25, 26]. The reconstructed density matrices for the singlet Bell state (Ψ^-) at signal (idler) wavelengths ranging from 693 nm to 682 nm (795 nm to 809.5 nm) are plotted in Fig. 3, with $F \geq 97\%$ for all wavelengths studied. The easily and broadly tunable wavelength of our source is a particularly unique and useful advantage for quantum-information applications.

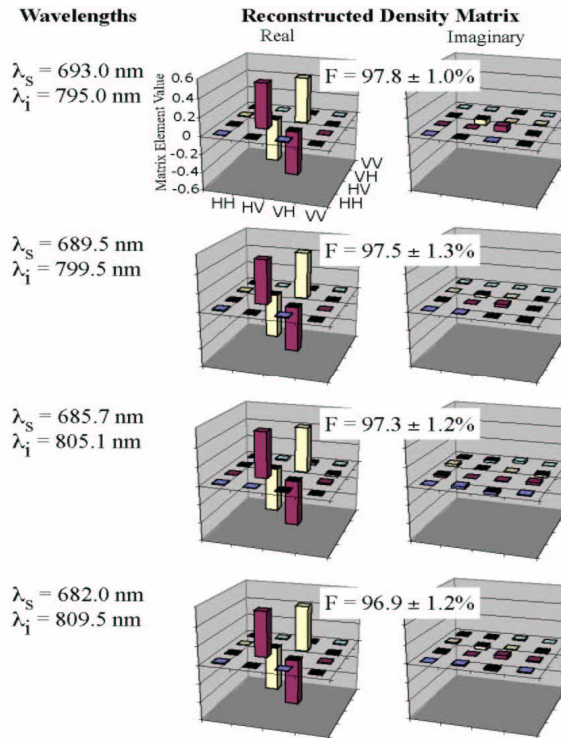


Fig. 3. Density matrix reconstruction of Bell state Ψ' produced at different wavelengths. The reconstructed density matrices are shown along with the fidelities calculated from the reconstructed matrices.

In addition to the advantages already discussed, the gain and dispersion of microstructure fiber can be controlled through design of the fiber's physical structure, such as the core size and air-hole size, as well as by choosing materials with higher nonlinearity. This should enable even higher two-photon production rates with lower background, as well as allowing pair production at wavelengths ranging from ultraviolet to infrared, meeting the requirements of more quantum-information applications. Although in an early development stage, this bright, phase-stable, wavelength tunable, single-mode fiber-based source of polarization-entangled photon pairs is already comparable to the best performing down-conversion-based sources. With its wavelength tunability and inherent mechanical stability, this source is a promising candidate for use in practical, real-world, quantum-information science applications.

Acknowledgments

This work has been supported in part by the Intelligence Advanced Research Projects Activity (IARPA) entangled photon source program, and the Multidisciplinary University Research Initiative Center for Photonic Quantum Information Systems (Army Research Office/IARPA program DAAD19-03-1-0199). M.D.E. acknowledges support from the National Research Council Postdoctoral Research Associateship Program.